so that the free density matrix solves the differential equation (3.42).

In this book, we shall be interested only in the density matrix in statistical mechanics, shown in eqn (3.41), which is related to the evolution operator in real time, $\mathrm{e}^{-\mathrm{i}tH}$. Formally, we can pass from real time t to inverse temperature β through the replacement

$$\beta = \mathrm{i}t,$$

and β is often referred to as an "imaginary" time. The quantum Monte Carlo methods in this chapter and in Chapter 4 usually do not carry over to real-time quantum dynamics, because the weights would become complex numbers, and could then no longer be interpreted as probabilities.

3.3 The Feynman path integral

In matrix squaring, one of the subjects of Section 3.2, we convolute two density matrices at temperature T to produce the density matrix at temperature $T/2$. By iterating this process, we can obtain the density matrix at any temperature from the quasi-classical high-temperature limit. Most often, however, it is impossible to convolute two density matrices analytically. With increasing numbers of particles and in high dimensionality, the available computer memory soon becomes insufficient even to store a reasonably discretized matrix $\rho(\mathbf{x}, \mathbf{x}', \beta)$, so that one cannot run Alg. 3.3 (`matrix-square`) on a discretized approximation of the density matrix. Monte Carlo methods are able to resolve this problem. They naturally lead to the Feynman path integral for quantum systems and to the idea of path sampling, as we shall see in the present section.

Instead of evaluating the convolution integrals one after the other, as is done in matrix squaring, we can write them out all together:

$$\begin{aligned}\rho(x, x', \beta) &= \int \mathrm{d}x''\ \rho(x, x'', \beta/2)\, \rho(x'', x', \beta/2) \\ &= \iiint \mathrm{d}x''\mathrm{d}x'''\mathrm{d}x''''\rho(x, x''', \frac{\beta}{4})\, \rho(x''', x'', \frac{\beta}{4})\, \rho(x'', x'''', \frac{\beta}{4})\, \rho(x'''', x', \frac{\beta}{4}) \\ &= \dots .\end{aligned}$$

This equation continues to increasingly deeper levels, with the kth applications of the matrix-squaring algorithm corresponding to $\simeq 2^k$ integrations. Writing $\{x_0, x_1, \dots\}$ instead of the cumbersome $\{x, x', x'', \dots\}$, this gives

$$\begin{aligned}\rho(x_0, x_N, \beta) = \int \cdots \int \mathrm{d}x_1 \dots \mathrm{d}x_{N-1} \\ \times \rho\left(x_0, x_1, \frac{\beta}{N}\right) \dots \rho\left(x_{N-1}, x_N, \frac{\beta}{N}\right), \quad (3.43)\end{aligned}$$

where we note that, for the density matrix $\rho(x_0, x_N, \beta)$, the variables x_0 and x_N are fixed on both sides of eqn (3.43). For the partition function,

there is one more integration, over the variable x_0, which is identified with x_N:

$$Z = \int \mathrm{d}x_0 \; \rho(x_0, x_0, \beta) = \int \cdots \int \mathrm{d}x_0 \ldots \mathrm{d}x_{N-1} \times \rho\left(x_0, x_1, \frac{\beta}{N}\right) \ldots \rho\left(x_{N-1}, x_0, \frac{\beta}{N}\right). \quad (3.44)$$

The sequence $\{x_0, \ldots, x_N\}$ in eqns (3.43) and (3.44) is called a path, and we can imagine the variable x_k at the value $k\beta/N$ of the imaginary-time variable τ, which goes from 0 to β in steps of $\Delta_\tau = \beta/N$ (see Feynman (1972)). Density matrices and partition functions are thus represented as multiple integrals over paths, called path integrals, both at finite N and in the limit $N \to \infty$. The motivation for this representation is again that for large N, the density matrices under the multiple integral signs are at small $\Delta_\tau = \beta/N$ (high temperature) and can thus be replaced by their quasi-classical high-temperature approximations. To distinguish between the density matrix with fixed positions x_0 and x_N and the partition function, where one integrates over $x_0 = x_N$, we shall refer to the paths in eqn (3.43) as contributing to the density matrix $\rho(x_0, x_N, \beta)$, and to the paths in eqn (3.44) as contributing to the partition function.

After presenting a naive sampling approach in Subsection 3.3.1, we discuss direct path sampling using the Lévy construction, in Subsection 3.3.2. The closely related later Subsection 3.5.1 introduces path sampling in Fourier space.

3.3.1 Naive path sampling

The Feynman path integral describes a single quantum particle in terms of paths $\{x_0, \ldots, x_N\}$ (often referred to as world lines), with weights given by the high-temperature density matrix or another suitable approximation:

$$Z = \underbrace{\int \int \mathrm{d}x_0, \ldots, \mathrm{d}x_{N-1}}_{\text{sum of paths}} \underbrace{\rho(x_0, x_1, \Delta_\tau) \cdot \cdots \cdot \rho(x_{N-1}, x_0, \Delta_\tau)}_{\text{weight } \pi \text{ of path}}.$$

More generally, any variable x_k can represent a d-dimensional quantum system. The full path then lies in $d+1$ dimensions.

Let us first sample the paths contributing to the partition function of a harmonic oscillator using a local Markov-chain algorithm (see Fig. 3.9). We implement the Trotter formula, as we would for an arbitrary potential. Each path comes with a weight containing terms as the following:

$$\underbrace{\ldots \rho^{\text{free}}(x_{k-1}, x_k, \Delta_\tau)\, \mathrm{e}^{-\frac{1}{2}\Delta_\tau V(x_k)}}_{\rho(x_{k-1}, x_k, \Delta_\tau) \text{ in Trotter formula}} \underbrace{\mathrm{e}^{-\frac{1}{2}\Delta_\tau V(x_k)} \rho^{\text{free}}(x_k, x_{k+1}, \Delta_\tau) \ldots .}_{\rho(x_k, x_{k+1}, \Delta_\tau) \text{ in Trotter formula}}$$

As shown, each argument x_k appears twice, and any two contributions $\exp\left[-\frac{1}{2}\Delta_\tau V(x_k)\right]$, where $V(x) = \frac{1}{2}x^2$, can be combined into a single

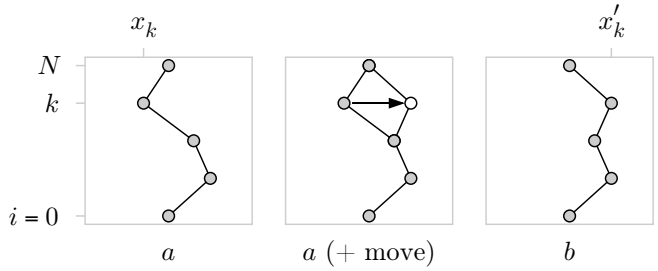

Fig. 3.9 Naive path-sampling move. The ratio π_b/π_a is computed from $\{x_{k-1}, x_k, x_{k+1}\}$ and from the new position x'_k.

term $\exp[-\Delta_\tau V(x_k)]$. To move from one position of the path to the next, we choose a random element k and accept the move $x_k \to x_k + \delta_x$ using the Metropolis algorithm. The ratio of the weights of the new and the old path involves only two segments of the path and one interaction potential (see Alg. 3.4 (`naive-harmonic-path`)). A move of x_k, for $k \neq 0$, involves segments $\{x_{k-1}, x_k\}$ and $\{x_k, x_{k+1}\}$. Periodic boundary conditions in the τ-domain have been worked in: for $k = 0$, we consider the density matrices between $\{x_{N-1}, x_0\}$ and $\{x_0, x_1\}$. Such a move across the horizon $k = 0$ changes x_0 and x_N, but they are the same (see the iteration $i = 10$ in Fig. 3.11).

procedure `naive-harmonic-path`
input $\{x_0, \ldots, x_{N-1}\}$
$\Delta_\tau \leftarrow \beta/N$
$k \leftarrow \texttt{nran}\,(0, N-1)$
$k_\pm \leftarrow k \pm 1$
if $(k_- = -1) k_- \leftarrow N$
$x'_k \leftarrow x_k + \texttt{ran}\,(-\delta, \delta)$
$\pi_a \leftarrow \rho^{\text{free}}\left(x_{k_-}, x_k, \Delta_\tau\right) \rho^{\text{free}}\left(x_k, x_{k_+}, \Delta_\tau\right) \exp\left(-\frac{1}{2}\Delta_\tau x_k^2\right)$
$\pi_b \leftarrow \rho^{\text{free}}\left(x_{k_-}, x'_k, \Delta_\tau\right) \rho^{\text{free}}\left(x'_k, x_{k_+}, \Delta_\tau\right) \exp\left(-\frac{1}{2}\Delta_\tau x_k'^2\right)$
$\Upsilon \leftarrow \pi_b/\pi_a$
if $(\texttt{ran}\,(0,1) < \Upsilon) x_k \leftarrow x'_k$
output $\{x_0, \ldots, x_{N-1}\}$

Algorithm 3.4 `naive-harmonic-path`. Markov-chain sampling of paths contributing to $Z^{\text{h.o.}} = \int \mathrm{d}x_0\ \rho^{\text{h.o.}}(x_0, x_0, \beta)$.

Algorithm 3.4 (`naive-harmonic-path`) is an elementary path-integral Monte Carlo program. To test it, we can generate a histogram of positions for any of the x_k (see Fig. 3.10). For large N, the error in the Trotter formula is negligible. The histogram must then agree with the analytical result for the probability $\pi(x) = \rho^{\text{h.o.}}(x, x, \beta)/Z$, which we can also calculate from eqns (3.38) and (3.40). This simple path-integral

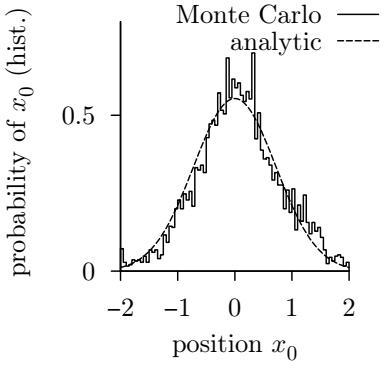

Fig. 3.10 Histogram of positions x_0 (from Alg. 3.4 (`naive-harmonic-path`), with $\beta = 4$, $N = 8$, and 1×10^6 iterations).

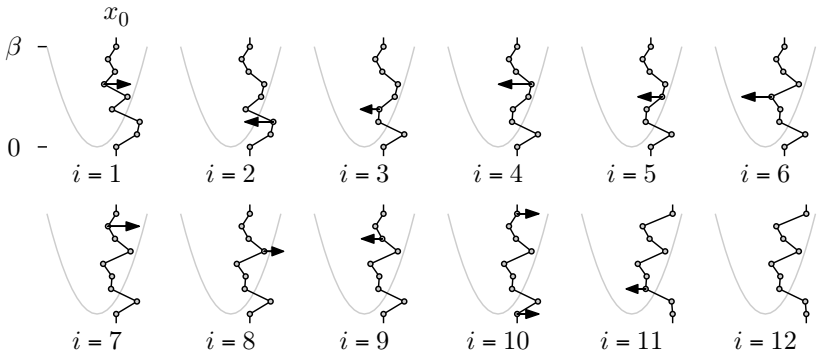

Fig. 3.11 Markov-chain path sampling for a harmonic potential (from Alg. 3.4 (`naive-harmonic-path`)).

Monte Carlo program can in principle, but rarely in practice, solve problems in equilibrium quantum statistical physics.

Algorithm 3.4 (`naive-harmonic-path`), like local path sampling in general, is exceedingly slow. This can be seen from the fluctuations in the histogram in Fig. 3.10 or in the fact that the path positions in Fig. 3.11 are all on the positive side ($x_k > 0$), just as in the initial configuration: Evidently, a position x_k cannot get too far away from x_{k-1} and x_{k+1}, because the free density matrix then quickly becomes very small. Local path sampling is unfit for complicated problems.

3.3.2 Direct path sampling and the Lévy construction

To overcome the limitations of local path sampling, we must analyze the origin of the high rejection rate. As discussed in several other places in this book, a high rejection rate signals an inefficient Monte Carlo algorithm, because it forces us to use small displacements δ. This is what happens in Alg. 3.4 (`naive-harmonic-path`). We cannot move x_k very far away from its neighbors, and are also prevented from moving larger parts of the path, consisting of positions $\{x_k, \ldots, x_{k+l}\}$. For concreteness, we first consider paths contributing to the density matrix of a free particle, and later on the paths for the harmonic oscillator. Let us sample the integral

$$\rho^{\text{free}}(x_0, x_N, \beta) = \int \cdots \int \mathrm{d}x_1 \ldots \mathrm{d}x_{N-1} \underbrace{\rho^{\text{free}}(x_0, x_1, \Delta_\tau)\, \rho^{\text{free}}(x_1, x_2, \Delta_\tau) \ldots \rho^{\text{free}}(x_{N-1}, x_N, \Delta_\tau)}_{\pi(x_1, \ldots, x_{N-1})}. \quad (3.45)$$

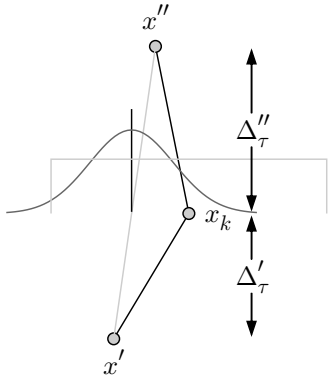

Fig. 3.12 Proposed and accepted moves in Alg. 3.4 (`naive-harmonic-path`). The position x_k is restrained by x' and x''.

We focus for a moment on Monte Carlo moves where all positions except x_k are frozen, in particular x_{k-1} and x_{k+1}. Slightly generalizing the problem, we focus on a position x_k sandwiched in between fixed positions

x' and x'', with two intervals in τ, Δ'_τ and Δ''_τ (see Fig. 3.12). In the naive path-sampling algorithm, the move is drawn randomly between $-\delta$ and $+\delta$, around the current position x_k (see Fig. 3.12). The distribution of the accepted moves in Fig. 3.12 is given by

$$\pi^{\text{free}}(x_k|x',x'') \propto \rho^{\text{free}}(x',x_k,\Delta'_\tau)\,\rho^{\text{free}}(x_k,x'',\Delta''_\tau)\,,$$

where

$$\rho^{\text{free}}(x',x_k,\Delta'_\tau) \propto \exp\left[-\frac{(x'-x_k)^2}{2\Delta'_\tau}\right],$$
$$\rho^{\text{free}}(x_k,x'',\Delta''_\tau) \propto \exp\left[-\frac{(x_k-x'')^2}{2\Delta''_\tau}\right].$$

Expanding the squares and dropping all multiplicative terms independent of x_k, we find the following for the probability of x_k:

$$\underline{\pi^{\text{free}}(x_k|x',x'')} \propto \exp\left(-\frac{\cancel{x'^2} - 2x'x_k + x_k^2}{2\Delta'_\tau} - \frac{x_k^2 - 2x_k x'' + \cancel{x''^2}}{2\Delta''_\tau}\right)$$
$$\propto \underline{\exp\left[-\frac{(x_k-\langle x_k\rangle)^2}{2\sigma^2}\right]}, \quad (3.46)$$

where

$$\langle x_k\rangle = \frac{\Delta''_\tau x' + \Delta'_\tau x''}{\Delta'_\tau + \Delta''_\tau}$$

and

$$\sigma^2 = (1/\Delta''_\tau + 1/\Delta'_\tau)^{-1}.$$

The mismatch between the proposed moves and the accepted moves generates the rejections in the Metropolis algorithm. We could modify the naive path-sampling algorithm by choosing x_k from a Gaussian distribution with the appropriate parameters (taking $x' \equiv x_{k-1}$ (unless $k=0$), $x'' \equiv x_{k+1}$, and $\Delta'_\tau = \Delta''_\tau = \beta/N$). In this way, no rejections would be generated.

The conditional probability in eqn (3.46) can be put to much better use than just to suppress a few rejected moves in a Markov-chain algorithm. In fact, $\pi^{\text{free}}(x_k|x',x'')$ gives the weight of all paths which, in Fig. 3.12, start at x', pass through x_k and end up at x''. We can sample this distribution to obtain x_1 (using $x' = x_0$ and $x'' = x_N$). Between the freshly sampled x_1 and x_N, we may then pick x_2, and thereafter x_3 between x_2 and x_N and, eventually, the whole path $\{x_1,\ldots,x_N\}$ (see Fig. 3.14 and Alg. 3.5 (`levy-free-path`)). A directly sampled path with $N = 50\,000$ is shown in Fig. 3.13; it can be generated in a split second, has no correlations with previous paths, and its construction has caused no rejections. In the limit $N\to\infty$, $x(\tau)$ is a differentiable continuous function of τ, which we shall further analyze in Section 3.5.

Direct path sampling—usually referred to as the Lévy construction—was introduced by Lévy (1940) as a stochastic interpolation between points x_0 and x_N. This generalizes interpolations using polynomials, trigonometric functions (see Subsection 3.5.1), splines, etc. The Lévy

Fig. 3.13 A path contributing to $\rho^{\text{free}}(x_0,x_N,\beta)$ (from Alg. 3.5 (`levy-free-path`), with $N = 50\,000$).

construction satisfies a local construction principle: the path $x(\tau)$, in any interval $[\tau_1, \tau_2]$, is the stochastic interpolation of its end points $x(\tau_1)$ and $x(\tau_2)$, but the behavior of the path outside the interval plays no role.

The Lévy construction is related to the theory of stable distributions, also largely influenced by Lévy (see Subsection 1.4.4), essentially because Gaussians, which are stable distributions, are encountered at each step. The Lévy construction can be generalized to other stable distributions, but it then would not generate a continuous curve in the limit $\Delta_\tau \to 0$.

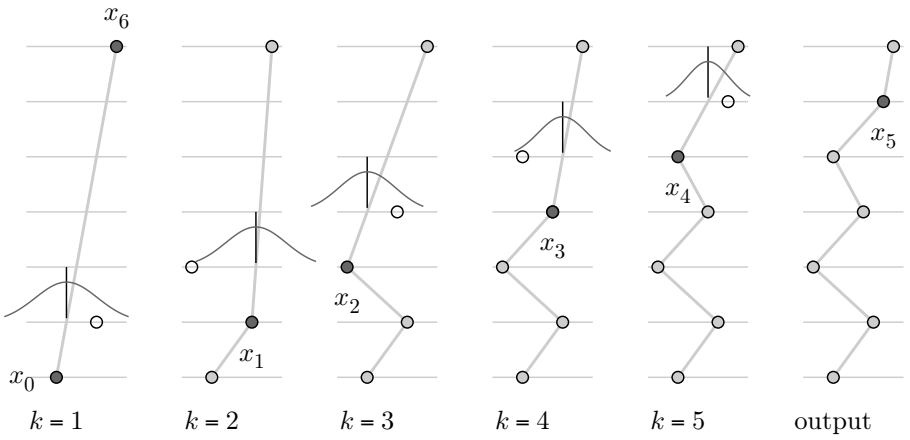

Fig. 3.14 Lévy construction of a free-particle path from x_0 to x_6 (see Alg. 3.5 (`levy-free-path`)).

procedure `levy-free-path`
input $\{x_0, x_N\}$
$\Delta_\tau \leftarrow \beta/N$
for $k = 1, \ldots, N-1$ **do**
$\quad \Delta'_\tau \leftarrow (N-k)\Delta_\tau$
$\quad \langle x_k \rangle \leftarrow (\Delta'_\tau x_{k-1} + \Delta_\tau x_N)/(\Delta_\tau + \Delta'_\tau)$
$\quad \sigma^{-2} \leftarrow \Delta_\tau^{-1} + \Delta_\tau'^{-1}$
$\quad x_k \leftarrow \langle x_k \rangle + \mathtt{gauss}\,(\sigma)$
output $\{x_0, \ldots, x_N\}$

Algorithm 3.5 `levy-free-path`. Sampling a path contributing to $\rho^{\mathrm{free}}(x_0, x_N, \beta)$, using the Lévy construction (see Fig. 3.14).

We now consider the Lévy construction for a harmonic oscillator. The algorithm can be generalized to this case because the harmonic density matrix is a Gaussian (the exponential of a quadratic polynomial), and the convolution of two Gaussians is again a Gaussian:

$$\rho^{\mathrm{h.o.}}(x', x'', \Delta'_\tau + \Delta''_\tau) = \int \mathrm{d}x_k \underbrace{\rho^{\mathrm{h.o.}}(x', x_k, \Delta'_\tau)\, \rho^{\mathrm{h.o.}}(x_k, x'', \Delta''_\tau)}_{\pi^{\mathrm{h.o.}}(x_k | x', x'')}.$$

Because of the external potential, the mean value $\langle x_k \rangle$ no longer lies on the straight line between x' and x''. From the nondiagonal harmonic density matrix in eqn (3.37), and proceeding as in eqn (3.46), we find the following:

$$\pi^{\text{h.o.}}(x_k|x',x'') \propto \exp\left[-\frac{1}{2\sigma^2}\left(x_k - \langle x_k \rangle\right)^2\right],$$

with parameters

$$\begin{aligned}
\langle x_k \rangle &= \frac{\Upsilon_2}{\Upsilon_1}, \\
\sigma &= \Upsilon_1^{-1/2}, \\
\Upsilon_1 &= \coth\ \Delta'_\tau + \coth\ \Delta''_\tau, \\
\Upsilon_2 &= \frac{x'}{\sinh \Delta'_\tau} + \frac{x''}{\sinh \Delta''_\tau},
\end{aligned}$$

as already used in the analytic matrix squaring for the harmonic oscillator. We can thus directly sample paths contributing to the harmonic density matrix $\rho^{\text{h.o.}}(x_0, x_N, \beta)$ (see Alg. 3.6 (`levy-harmonic-path`)), and also paths contributing to $Z^{\text{h.o.}} = \int \mathrm{d}x_0\ \rho^{\text{h.o.}}(x_0, x_0, \beta)$, if we first sample x_0 from the Gaussian diagonal density matrix in eqn (3.38).

procedure `levy-harmonic-path`
input $\{x_0, x_N\}$
$\Delta_\tau \leftarrow \beta/N$
for $k = 1, \ldots, N-1$ **do**
$$\left\{\begin{array}{l}
\Upsilon_1 \leftarrow \coth \Delta_\tau + \coth\left[(N-k)\Delta_\tau\right] \\
\Upsilon_2 \leftarrow x_{k-1}/\sinh \Delta_\tau + x_N/\sinh\left[(N-k)\Delta_\tau\right] \\
\langle x_k \rangle \leftarrow \Upsilon_2/\Upsilon_1 \\
\sigma \leftarrow 1/\sqrt{\Upsilon_1} \\
x_k \leftarrow \langle x_k \rangle + \texttt{gauss}\,(\sigma)
\end{array}\right.$$
output $\{x_0, \ldots, x_N\}$

Algorithm 3.6 `levy-harmonic-path`. Sampling a path contributing to $\rho^{\text{h.o.}}(x_0, x_N, \beta)$, using the Lévy construction (see Fig. 3.15).

In Alg. 3.5 (`levy-free-path`), we were not obliged to sample the path in chronological order (first x_0, then x_1, then x_2, etc.). After fixing x_0 and x_N, we could have chosen to sample the midpoint $x_{N/2}$, then the midpoint between x_0 and $x_{N/2}$ and between $x_{N/2}$ and x_N, etc. (see Alg. 3.8 (`naive-box-path`) and Fig. 3.19 later). We finally note that free paths can also be directly sampled using Fourier-transformation methods (see Subsection 3.5.1).

3.3.3 Periodic boundary conditions, paths in a box

We now turn to free paths in a box, first with periodic boundary conditions, and then with hard walls. A path contributing to the density